Persistent changes in neuronal structure and synaptic plasticity caused by proton irradiation

Vipan K. Parihar, **Junaid Pasha**, **Katherine K. Tran**, **Brianna M. Craver**, **Munjal M. Acharya**, and **Charles L. Limoli**[1]
Department of Radiation Oncology, University of California, Irvine, CA 92697-2695, USA

Abstract

Cranial radiotherapy is used routinely to control the growth of primary and secondary brain tumors, but often results in serious and debilitating cognitive dysfunction. In part due to the beneficial dose depth distributions that may spare normal tissue damage, the use of protons to treat CNS and other tumor types is rapidly gaining popularity. Astronauts exposed to lower doses of protons in the space radiation environment are also at risk for developing adverse CNS complications. To explore the consequences of whole body proton irradiation, mice were subjected to 0.1 and 1 Gy and analyzed for morphometric changes in hippocampal neurons 10 and 30 days following exposure. Significant dose-dependent reductions (~33%) in dendritic complexity were found, when dendritic length, branching and area were analyzed 30 days after exposure. At equivalent doses and times, significant reductions in the number (~30%) and density (50–75%) of dendritic spines along hippocampal neurons of the dentate gyrus were also observed. Immature spines (filopodia, long) exhibited the greatest sensitivity (1.5–3 fold) to irradiation, while more mature spines (mushroom) were more resistant to changes over a 1-month post-irradiation timeframe. Irradiated granule cell neurons spanning the subfields of the dentate gyrus showed significant and dose-responsive reductions in synaptophysin expression, while the expression of postsynaptic density protein (PSD-95) was increased significantly. These findings corroborate our past work using photon irradiation, and demonstrate for the first time, dose-responsive changes in dendritic complexity, spine density and morphology and synaptic protein levels following exposure to low dose whole body proton irradiation.

Keywords

Introduction

Exposure of the central nervous system (CNS) to ionizing radiation, either clinically for the control of cancer or through occupational scenarios elicits varying degrees of normal tissue

---

[1]**Corresponding author**: Prof. Charles L. Limoli, Department of Radiation Oncology, University of California Irvine, Medical Sciences I, Room B-146B, Irvine CA 92697-2695, USA. phone: (949) 824-3053, Fax: (949) 824-3566, climoli@uci.edu.
The authors declare no conflicts of interest

damage that carries the risk of compromising cognitive function. While radiotherapy can effectively limit primary and secondary tumor growth in the brain, increased survival is often associated with severe neurocognitive sequelae (Butler et al. 2006; Gorlia et al. 2012; Meyers 2000; Saury and Emanuelson 2011). Substantial evidence has now linked cranial irradiation to progressive and debilitating cognitive dysfunction (Barani et al. 2007). The effects of irradiation disrupt diverse cognitive functions including learning, memory, processing speed, attention and executive function (Meyers 2000). In part by efforts designed to minimize the adverse and unintended side effects of radiotherapy, the use of protons for clinical radiotherapy is rapidly expanding. Outside of the clinical setting, new research in rodents have identified similar adverse cognitive effects resulting from exposure to charged particles typical of the space radiation environment (Britten et al. 2012; Lonart et al. 2012; Tseng et al. 2013). Thus, whether at lower or higher dosing paradigms, exposure of the CNS is associated with an increased risk of developing acute and longer-term cognitive decrements (Greene-Schloesser et al. 2012; Lonart et al. 2012). The foregoing has become an increasing concern for those exposed under a variety of scenarios, not only due to the increasing numbers of cancer survivors, but also due to the conspicuous lack of any satisfactory long-term solutions for this serious side effect of radiation exposure to the CNS.

While the mechanisms linking radiation damage to cognitive dysfunction remain uncertain, increasing evidence suggests that persistent elevations in secondary reactive oxygen and nitrogen and inflammatory species play a contributory if not causal role in hastening the onset and/or severity of cognitive impairment. Oxidative and inflammatory processes are elevated in a number of neurodegenerative conditions such as Alzheimer's disease (Markesbery 1997), Parkinson's disease (Zhou et al. 2008), amyotrophic lateral sclerosis (D'Amico et al. 2013) and can contribute to the persistent inhibition of hippocampal neurogenesis following irradiation (Mizumatsu et al. 2003; Limoli et al. 2007; Fike et al. 2009). Despite the impact of neurogenesis on cognition, it contributes a relatively small percentage of neurons that functionally integrate into functional synaptic circuits (van Praag et al. 2002), suggesting that other factors may be important for radiation-induced cognitive dysfunction.

To pursue the foregoing, and based on the absence of quantitative information regarding the impact of irradiation on mature neuronal structures, studies were undertaken to analyze acute and longer-term changes in the morphometric properties of irradiated neurons. Significant evidence has linked compromised dendritic and spine morphology to a host of neurodegenerative disorders (Kaufmann and Moser 2000; Huttenlocher 1991; Kolb and Whishaw 1998; Tronel et al. 2010). Dendritic abnormalities are commonplace among diseases as epilepsy (Imitola et al. 2004), recurrent depressive illness (Bremner et al. 1995), Alzheimer's disease (Terry et al. 1981) and Huntington's disease (Kaufmann and Moser 2000), and correlate with intellectual disabilities found in Down's (Takashima et al. 1994), Rett syndrome (Armstrong et al. 1998) and Fragile -X syndromes (Kaufmann and Moser 2000).

Given the importance of structure function relationships in the CNS, it's not unexpected that optimal CNS connectivity depends on the growth, branching, pruning and remodeling of dendrites and spines to link activity dependent synaptogenesis to the dynamic needs of the

CNS. Our past findings showing radiation-induced reductions in dendritic spine densities and morphologies (Parihar and Limoli 2013) parallel similar findings that suggest agents or conditions that lead to reduced spine densities or perturbed morphology predispose individuals to developing cognitive impairments (Pfeiffer and Huber 2009; Selkoe 2002; Yuste and Bonhoeffer 2001, 2004; van Spronsen and Hoogenraad 2010).

The foregoing indicates that changes in the ultrastructural features of neurons are critical determinants for learning and memory, and when disruptions to these intricate structural elements occur, cognitive function begins to deteriorate. The capability of gamma irradiation to precipitate long lasting changes in synaptic plasticity that resemble many neurodegenerative conditions suggested such changes might underlie many of the resultant cognitive defects. Based on the increasing presence of hadron therapy for the treatment of CNS and other malignancies (Miller et al. 2012), and the paucity of information regarding the effects of such treatments on neuronal structure, we sought to determine if/how exposure to energetic protons might elicit acute and chronic alterations to the anatomical structure of neurons. To facilitate our neurobiologic studies of radiation effects, we selected a transgenic mouse model that expresses enhanced green fluorescent protein (eGFP) under the control of a modified Thy1 promoter that restricts expression to certain subsets of neurons. With this model, we report our findings detailing the consequences of proton irradiation on neuronal micromorphometric parameters, including dendritic anatomy, spine morphology and synaptic density.

Materials and Methods

Animals, proton irradiation and tissue harvesting

All animal procedures were carried out in accordance with NIH and IACUC guidelines. Transgenic mice [strain Tg(Thy1-EGFP)MJrsJ, Stock No. 007788, Jackson Laboratory, CT, USA] harboring the *Thy1-EGFP* transgene were housed in ventilated cages, fed a standard pelleted rodent chow, and housed in an environmentally controlled room with a 14:10-h light: dark cycle. Mice were bred and genotyped to confirm the presence of *Thy1-EGFP* transgene. Male mice positive for the *Thy1-EGFP* transgene were used for all studies.

Two months old mice were exposed to whole body proton irradiation (0.1 or 1 Gy). Proton irradiations were conducted at the Loma Linda University (CA, USA) Proton Research Facility synchrotron accelerator using 250 MeV plateau phase protons delivered at a dose rate of 0.25 Gy/min. Following irradiation mice were returned to housing until the time of analysis. Mice were sacrificed at day 10 or 30 post-irradiation by transcardial perfusion, after which brains were cryoprotected and sectioned coronally (30 or 100μm thick) as described previously (Parihar and Limoli 2013).

Immunohistochemistry and quantification pre- and postsynaptic protein levels

Coronal sections (30μm thick) were immunostained for the quantification of postsynaptic density protein (PSD-95) or the presynaptic marker synaptophysin as described previously (Parihar and Limoli 2013). Briefly, serial 30μm-thick sections (3/animal) from the anterior to posterior hippocampus were selected, and 3 different fields (220 μm×220μm) in each

section were imaged from the dentate gyrus. Images were collected using a Nikon Eclipse TE 2000-U microscope with 0.5 μm-interval high-resolution z-stacks (1024×1024 pixel). Analysis of PSD-95 or synaptophysin was performed using the IMARIS spot tool (v7.6, Bitplane Inc., Switzerland) that detects immunostained puncta within 3D deconvoluted image stacks. Puncta satisfying pre-defined criteria (verified visually for accuracy) are converted to spots for quantification under preset parameters kept constant throughout subsequent analyses (Parihar and Limoli 2013).

Confocal microscopy, imaging and image processing

The expression of eGFP within neurons of homozygous or hemizygous *Thy1-EGFP* mice provides a brightly fluorescent signal that expedites the micromorphometric analyses of specific neuronal subsets. The strong signal to noise ratio of the fluorescent neurons provides for an accurate, precise and rigorous analysis and quantification of the complete dendritic tree. For dendritic analyses, 100μm thick hippocampal sections were prepared for confocal imaging. Three sections per animal were used to generate Z-stacks from 4 animals using a Nikon Eclipse TE 2000-U microscope (Nikon, Japan). Images comprising each Z-stack (1024×1024 pixels) were acquired at (40×) over the entire dendrite tree at 0.5μm increments. Quantification of dendritic parameters was derived from Z-stacks reconstructed in 3D from deconvoluted images using the AutoQuantX3 algorithm (MediaCybernetics, MD, USA). Deconvoluted 3D reconstructions yielded high spatial resolution images for detailed dendritic tracing and spine classification using the IMARIS software suite (Bitplane Inc.) as previously described (Parihar and Limoli 2013).

Neuron reconstruction and spine classification

Details regarding the reconstruction of neurons and the morphologic classification of spines have been described (Parihar and Limoli 2013). Briefly, an algorithm for tracing dendritic filament was used to reconstruct the entire dendritic tree spanning a series of Z-stacks (220×220 μm^2). Dendritic tracing originates from the soma (diameters 8–11μm) and terminates once dendrite diameters reach sizes less than 0.6μm. Reconstructed dendritic trees are then reanalyzed for dendritic spines that can be labeled, manually verified, morphologically categorized and quantified (Parihar and Limoli 2013). For spines to be included in our analyses a maximum spine length and minimum spine end diameter were set at 2.5 μm and 0.4μm, respectively. Parameters for the reconstruction and classification of dendrites and spines were selected after manual measurements from multiple neurons (8–10) from each cohort. Parameters were further validated from an independent series of pilot reconstructions in both manual and semi-automatic modes. Images were compared for accuracy and consistency to ensure that selected parameters represented actual variations in dendritic structure.

Statistical analyses

All morphological data in the present study are derived from 4 animals per group and presented as the Mean ± S.E.M. The differences in gross dendritic structure (*e.g.* total dendritic length) and all spine parameters were assessed by ANOVA (GraphPad Prism software, v6.0, IBM Inc., CA, USA). *P* values less than 0.05 were considered significant.

For multiple comparisons of dendritic and spine parameters, the Bonferroni correction was applied.

Results

Radiation-induced reductions in dendritic complexity

The inherent fluorescence of the eGFP expressing neurons in our selected transgenic mouse model provide for a detailed analysis of neuronal micromorphometry. Animals subjected to low (0.1 Gy) or higher (1 Gy) dose proton irradiation were analyzed over time for changes in dendritic complexity. Neurons analyzed in the granule cell layer (GCL) of the hippocampus exhibit significant dose-responsive reductions in dendritic complexity 10 or 30 days (Fig. 1, Tables S1, S2) following exposure. Radiation-induced reductions in dendritic complexity are readily apparent in deconvoluted (Fig. 1, A–C) and reconstructed (Fig. 1, D–F) images. Reconstructed images (9 total) were used to quantify changes in the number of dendritic branches, branch points, length and area when compared to unirradiated controls 10 or 30 days after irradiation (Fig. 1). While changes in the dendritic tree were less apparent at the 10 day time, reductions of all morphometric endpoints were significantly lower 30 days following the 1 Gy dose (Fig. 1). Compared to controls, mean values of dendritic branches (76%, $P<0.05$), branch points (65%, $P<0.05$), total length (61%, $P<0.05$), and total area (65 %, $P<0.01$) were markedly lower after 1 Gy (Fig. 1G–J).

Radiation-induced reductions in dendritic spines

Quantification of dendritic spines and spine morphology following proton irradiation was facilitated by the presence of brightly fluorescent GCL neurons. Analysis of several dendritic spine parameters 10 or 30 days following exposure revealed significant and persistent dose-responsive changes (Fig. 2, Tables S3, S4, S5). At 10 days post-irradiation, the higher dose (1 Gy) reduced significantly the number of spines by 31 % compared to controls ($P<0.001$, Fig. 2), an effect that persisted to day 30($P<0.001$, Fig. 2). Measurements of spine density confirmed similar trends at 10 days post-irradiation, where 1 Gy reduced spine density by 50% compared to controls ($P<0.01$, Fig. 2). These changes were markedly enhanced at the 30-day time point, where spine density was reduced significantly by 39% ($P<0.05$) and 70% ($P<0.01$) after 0.1 and 1.0 Gy respectively (Fig. 2). Spine volumes were relatively unaffected under the irradiation paradigms used (Fig. 2).

Radiosensitivity of immature spines

To determine whether morphologically distinct spines exhibit inherent differences in radiosensitivity, distinct subclasses of spines were categorized and quantified at 10 and 30 days following exposure (Fig. 3, Tables S6, S7). Reconstructed dendritic segments were analyzed for changes in specific subclasses of spines at different time after irradiation as shown in representative images (Fig. 3). Based on rigorous morphometric criteria (Parihar and Limoli 2013), dendritic spines were classified as either filopodia, long, mushroom or stubby. In general, more mature spines (mushroom) along GCL neurons were found to be relatively radioresistant, as their yields did not change significantly compared to unirradiated controls. However, irradiation had the largest impact on filopodia, where the yield of these relatively immature spines was significantly reduced by 66% ($P<0.001$) 10 days after 1.0 Gy

and by 64% (p<0.001) and 73% (p<0.001) 30 days after 0.1 or 1.0 Gy respectively (Fig. 3). Furthermore, 41% (p<0.05) reductions in the immature long spine morphologies were found 30 days after a 1.0 Gy dose of protons (Fig. 3). Evident from this data is that spines of defined morphology exhibit differential susceptibility to irradiation.

Radiation-induced up-regulation of postsynaptic density protein (PSD-95) in the dentate gyrus

To analyze the consequences of irradiation on synaptic protein levels in hippocampal neurons, immunohistochemistry was undertaken. Given the important role of the postsynaptic density protein (PSD-95) in regulating synaptic plasticity, we sought to analyze discrete immunostained puncta that can be visualized for deconvolution and quantification. Neurons analyzed in the GCL and molecular layer (ML) showed significant increases in the level of PSD-95 expression after each radiation dose when compared to controls 10 and 30 days post-irradiation (Fig. 4, Table S8A). The yield of PSD-95 puncta in the GCL and ML after 1 Gy increased significantly by 59% (*P*<0.05) when compared to controls 10 days later (Fig. 4). Interestingly, both 0.1 and 1.0 Gy proton doses led to significant (p<0.001) increases of 81% and 110% respectively in PSD-95 puncta compared to controls 30 days after irradiation (Fig. 4). These data clearly demonstrate that exposure to high energy protons can elevate the level of PSD-95 puncta over an extended period of time.

Radiation-induced down-regulation of the presynaptic protein synaptophysin in the dentate hilus

To determine the effects of proton irradiation on a pre-synaptic protein, immunohistochemistry was undertaken on the dentate hilus (DH), a hippocampal subfield enriched in presynaptic terminals. Similar to the studies above, synaptophysin expression in the form of discrete puncta was analyzed 10 and 30 days following irradiation by confocal microscopy (Fig. 5, Table S8B). In unirradiated controls, synaptophysin puncta were more abundant, with individual clusters containing greater numbers of puncta compared to irradiated samples. Reduced staining was evident by day 10 following irradiation and continued to dissipate throughout the dentate gyrus by day 30. At the earlier 10-day time, synaptophysin expression was reduced significantly in the DH by 30% (*P*<0.05) after 1.0 Gy compared to controls (Fig. 5). At the latter 30-day time, the expression of synaptophysin was still reduced significantly, lower by 24% (*P*<0.01) and 48% (*P*<0.001) after 0.1 and 1.0 Gy respectively when compared to controls (Fig. 5). These data again demonstrate that proton irradiation can induce a dose-responsive and persistent reduction in the levels of synaptophysin.

Discussion

In the present study we have undertaken a micromorphometric analysis of GCL neurons in the hippocampus of transgenic mice that express eGFP in specific neuronal subsets. We have recently reported the use of this system to characterize the impact of photon irradiation on this same region of the brain, where marked reductions in dendritic complexity were found to coincide with alterations in dendritic spine density and changes in synaptic proteins (Parihar and Limoli 2013). Following the same rigorous morphometric criteria, we have

now completed a comprehensive analysis of the consequences of hadron therapy on neurons within in discrete subfields of the hippocampus. While our analysis has revealed qualitatively similar trends between gamma and proton irradiation, important quantitative differences have also emerged. Significant and persistent reduction in ultrastructural features of GCL neurons coupled with alterations in pre- and postsynaptic protein levels are likely to hasten the onset and severity of neurocognitive sequelae resulting from exposure to highly energetic protons.

The expansion of proton therapy units across the US points to a future whereby a larger numbers of cancer survivors will be subject to normal tissue damage resulting from hadron rather than photon therapy. The differences between the dose-depth distributions between these two radiation modalities suggest that normal tissue sparing resulting from hadron therapy may ultimately reduce complications associated with radiotherapy (Mohan and Bortfeld 2011). Despite the potential benefits of protons in radiotherapy, and in particular for the CNS, little or no information has been reported regarding the impact of proton irradiation on the more intricate subcellular structures that define neuronal anatomy. The capability of photon irradiation to elicit significant perturbations to the neuronal architecture suggested that equivalent of even lower doses of protons may cause significant harm to existing circuits in the brain. The space radiation environment is another non-clinical setting where the CNS is routinely exposed to the variable fluences and energies of these charged particles, albeit at much lower doses (Cucinotta and Durante 2006; Durante and Cucinotta 2008). The foregoing provided much of the rationale for undertaking a series of studies to determine the consequences of relatively low dose proton exposure on the CNS.

As alluded to above, present findings indicate that proton irradiation (1 Gy) elicits a spectrum of fundamentally similar changes to GCL neurons in the hippocampus. Quantification of multiple morphometric parameters revealed significant reductions in dendritic complexity that were particularly evident 30 days following a single 1 Gy dose of protons (Fig. 1). Concomitant with the reductions in dendritic arborization were significantly lower numbers of dendritic spines that resulted in dose-responsive and persistent reductions in spine density (Fig. 2). Noteworthy among these findings was that even the low 0.1 Gy proton dose was sufficient to cause a significant drop in spine density 1 month afterwards. To further dissect the effects of proton irradiation, different spine morphologies were quantified along defined dendritic segments (Fig. 3). As observed with photon irradiation (Parihar and Limoli 2013), exposure to protons had less of an effect on mature compared to immature spines. At day 10 following exposure, only the higher dose of 1 Gy led to a significant reduction in filopodia, while the remaining spine types were relatively unaffected (Fig. 3). However, 30 days after irradiation, significant and dose responsive reductions in immature filopodia were found at both 0.1 and 1.0 Gy doses. Interestingly, and opposed to prior findings with photons, a 1.0 Gy dose of protons caused a significant drop in long spines (Fig. 3), suggesting the capability of protons to reduce the yield of long spines. Dendritic spines are the structural correlates of learning and memory that regulate synaptic plasticity through dynamic changes in connectivity that are intimately dependent on changes in dendritic arborization (Yoshihara et al. 2009). While some controversy exists regarding the precise function of specific spine types (Hermel et al. 2006; Urbanska et al. 2012), recent evidence suggests that thin spines are more plastic and involved in learning, while mature

spines play a larger role in memory (Bourne and Harris 2007). Changes in morphology or spine density that adversely impact synaptic function have been found to compromise neurotransmission and behavioral performance (Matsuzaki et al. 2004). Present and recent findings have now demonstrated that photons and protons over a wide range of doses can elicit persistent reductions in dendritic complexity and spine density. Because these changes resemble those defining several neurodegenerative conditions, results are consistent with the idea that radiation-induced dementia that progresses in brain cancer survivors (Butler et al. 2006; Greene-**Schloesser and Robbins 2012) is in part, caused by ultrastructural changes to neurons that persist over time.

To understand further how proton irradiation might modulate synaptic plasticity, we analyzed hippocampal neurons for alterations in pre-and postsynaptic proteins. Interestingly, the relatively low doses of protons used in this study were found to elicit significant and dose-responsive increases in PSD-95 levels. Expression of PSD-95 puncta were elevated across the GCL and ML subfields of the DG compared to controls, particularly at the 30 day post-irradiation time point (Fig. 4). These findings corroborate past work with photons (Parihar and Limoli 2013) and demonstrate that acute exposure to a wide range of doses stimulates a persistent increase in PSD-95 expression along the dendrites of hippocampal neurons. PSD-95 is involved in the development, outgrowth, branching and maturation of dendritic spines and also plays a role in modulating synaptic signals (Chen et al. 2010; Matsuzaki et al. 2004). While increased PSD95 levels might suggest more or larger synapses, dendritic spine morphology (Fig. 3) suggests the opposite. In healthy brains, elevated levels of PSD-95 enhance synapse formation and promote larger synapses. However, over expression of PSD-95 is also associated with aging, neuroinflamation and impaired cognitive function (Chugh et al. 2013; Preissmann et al. 2012; Urbanska et al. 2012). Furthermore, PSD-95 expression varies according to spine type and increases with spine maturation, being relatively low on immature filopodia and relatively high on mushroom spines (Yoshihara et al. 2009). Since we found a relatively small effect on the number of mature spines (mushroom) but significant radiation-induced reductions in the number of immature spines (filopodia), elevated PSD-95 may not be necessarily contradictory. Increased levels of PSD-95 could be related to the activation of excitatory synapses located on mushroom spines. In support of this, studies analyzing excitatory toxicities have found a correlation between elevated levels of PSD-95 and enhanced excitatory synaptic connectivity in neurons (Chugh et al. 2013). PSD-95 over expression may alter the ratio of excitatory to inhibitory synaptic contacts and hence neuronal excitability that underlie many complex psychiatric disorders (Levinson et al. 2005). Thus, radiation-induced elevations in PSD-95 are likely to alter neurotransmission through a variety of mechanisms including the inhibition dendritic branching and dendritogenesis that ultimately reduce the complexity of the dendritic tree.

Present studies conducted at pre-synaptic sites along the same neurons in the DH subfield of the hippocampus, revealed significant and dose-responsive reduction in the presynaptic marker synpatophysin. At 30 days following proton irradiation, synaptophysin levels were reduced significantly at 0.1 and 1.0 Gy, (Fig. 5), providing further support for the capability of low dose proton irradiation to hasten the degeneration of GCL neurons and disrupt the neurotransmission in the irradiated brain.

Present and past data has now uncovered convincing evidence that both photon and proton irradiation elicits persistent and adverse changes on the morphology of hippocampal neurons (Parihar and Limoli 2013). Proton irradiation led to significant and generally dose-responsive reductions in dendritic branching, spine density and alterations in spine morphology and synaptic proteins that likely disrupt basal neurotransmission through changes in synaptic plasticity. It is informative to compare morphometric endpoints measured after exposure to the different types of irradiation (photon versus proton) at the same dose (1 Gy) and post-irradiation intervals. A summary of this data (Table 1) reveals some interesting trends. Photon irradiation leads to an increased reduction of all dendritic parameters (branching, length, area) when compared to proton irradiation. At 10 days after photon exposure, overall dendritic complexity (all parameters) is reduced by an average of 30% compared to just 4.5% for protons. By 30 days, photon irradiation reduced dendritic complexity by an average of 61% compared to 35% for protons. This situation reverses however, when spines are analyzed, as protons were found to cause greater drops in spines numbers and density when compared to photons. Protons caused reductions in spine number and density of 31 and 50% respectively at day 10 compared to just 4 and 9% for photons. By day 30, protons led to reductions in spine number and density of 42 and 70% respectively, compared to 30 and 41% after photon exposure. These overall differences in spine numbers and density between photons and protons translated to significant changes in the number of filopodia and long spines observed after irradiation. While photons reduced filopodia by 4 and 40% at days 10 and 30 respectively, protons reduced these same spine morphologies by 66 and 73% respectively. Differences found between each radiation modality for synaptic protein levels were not as pronounced, although both photons and protons led to similar trends in PSD-95 (up-regulated) and synaptophysin (down-regulated) expression. In summary, exposure to proton irradiation leads to disruptions in dendritic morphology and spinogenesis that persist over time and are more pronounced than that found with photon irradiation. While it remains if/how these changes translate to cognitive deficits, similar low dose exposures using the same mouse background (C57Bl6) have confirmed that charged particle irradiation disrupts behavioral performance and leads to cognitive decrements (Tseng et al. 2013).

The foregoing suggests that the morphometric changes measured in the brains of mice exposed to proton irradiation will be contributory if not causal to radiation-induced dementia. Comparison of photon and proton data analyzed at the same post-irradiation times indicates a progressive degradation of dendritic architecture. As shown schematically (Fig. 6), subtle to severe changes in dendrite structure measured 10 after exposure, all progress to severe disruptions when analyzed 30 days post-irradiation. Persistent morphological disruptions to neurons lead to altered synaptic plasticity and neurotransmission that can manifest as cognitive dysfunction. The morphometric changes reported here are temporally coincident with other radiation-induced secondary reactive processes such as oxidative stress and inflammation, representing some of multiple factors capable of impacting cognition. Our study contributes significantly to ongoing efforts to define the radiation-induced changes that underlie cognitive dysfunction. We assert that the persistent reductions in dendritic complexity and spine density along with disruptions to spine morphology and

synaptic proteins collectively disrupt neurotransmission and CNS functionality in the irradiated brain.

Supplementary Material

Refer to Web version on PubMed Central for supplementary material.

Acknowledgments

References

Armstrong DD, Dunn K, Antalffy B. Decreased dendritic branching in frontal, motor and limbic cortex in Rett syndrome compared with trisomy 21. Journal of neuropathology and experimental neurology. 1998; 57(11):1013–1017. [PubMed: 9825937]

Barani IJ, Cuttino LW, Benedict SH, Todor D, Bump EA, Wu Y, Chung TD, Broaddus WC, Lin PS. Neural stem cell-preserving external-beam radiotherapy of central nervous system malignancies. Int J Radiat Oncol Biol Phys. 2007; 68(4):978–985. [PubMed: 17467925]

Bourne J, Harris KM. Do thin spines learn to be mushroom spines that remember? Curr Opin Neurobiol. 2007; 17(3):381–386. [PubMed: 17498943]

Bremner JD, Krystal JH, Southwick SM, Charney DS. Functional neuroanatomical correlates of the effects of stress on memory. Journal of traumatic stress. 1995; 8(4):527–553. [PubMed: 8564272]

Britten RA, Davis LK, Johnson AM, Keeney S, Siegel A, Sanford LD, Singletary SJ, Lonart G. Low (20 cGy) doses of 1 GeV/u (56)Fe--particle radiation lead to a persistent reduction in the spatial learning ability of rats. Radiat Res. 2012; 177(2):146–151. [PubMed: 22077338]

Butler JM, Rapp SR, Shaw EG. Managing the cognitive effects of brain tumor radiation therapy. Curr Treat Options Oncol. 2006; 7(6):517–523. [PubMed: 17032563]

Chen Y, Rex CS, Rice CJ, Dube CM, Gall CM, Lynch G, Baram TZ. Correlated memory defects and hippocampal dendritic spine loss after acute stress involve corticotropin-releasing hormone signaling. Proc Natl Acad Sci U S A. 2010; 107(29):13123–13128. [PubMed: 20615973]

Chugh D, Nilsson P, Afjei SA, Bakochi A, Ekdahl CT. Brain inflammation induces post-synaptic changes during early synapse formation in adult-born hippocampal neurons. Exp Neurol. 2013; 250:176–188. [PubMed: 24047952]

Cucinotta FA, Durante M. Cancer risk from exposure to galactic cosmic rays: implications for space exploration by human beings. The lancet oncology. 2006; 7(5):431–435. [PubMed: 16648048]

D'Amico E, Factor-Litvak P, Santella RM, Mitsumoto H. Clinical perspective on oxidative stress in sporadic amyotrophic lateral sclerosis. Free Radic Biol Med. 2013; 65C:509–527. [PubMed: 23797033]

Durante M, Cucinotta FA. Heavy ion carcinogenesis and human space exploration. Nature reviews Cancer. 2008; 8(6):465–472.

Fike JR, Rosi S, Limoli CL. Neural precursor cells and central nervous system radiation sensitivity. Semin Radiat Oncol. 2009; 19(2):122–132. doi:S1053-4296(08)00085-4 [pii] 10.1016/ j.semradonc.2008.12.003. [PubMed: 19249650]

Gorlia T, Stupp R, Brandes AA, Rampling RR, Fumoleau P, Dittrich C, Campone MM, Twelves CC, Raymond E, Hegi ME, Lacombe D, van den Bent MJ. New prognostic factors and calculators for outcome prediction in patients with recurrent glioblastoma: a pooled analysis of EORTC Brain Tumour Group phase I and II clinical trials. Eur J Cancer. 2012; 48(8):1176–1184. [PubMed: 22464345]

Greene-Schloesser D, Robbins ME. Radiation-induced cognitive impairment--from bench to bedside. Neuro-oncology. 2012; 14(Suppl 4):iv37–iv44. [PubMed: 23095829]

Greene-Schloesser D, Robbins ME, Peiffer AM, Shaw EG, Wheeler KT, Chan MD. Radiation-induced brain injury: A review. Frontiers in oncology. 2012; 2:73. [PubMed: 22833841]

Hermel EE, Faccioni-Heuser MC, Marcuzzo S, Rasia-Filho AA, Achaval M. Ultrastructural features of neurons and synaptic contacts in the posterodorsal medial amygdala of adult male rats. Journal of anatomy. 2006; 208(5):565–575. [PubMed: 16637879]

Huttenlocher PR. Dendritic and synaptic pathology in mental retardation. Pediatric neurology. 1991; 7(2):79–85. [PubMed: 2059260]

Imitola J, Raddassi K, Park KI, Mueller FJ, Nieto M, Teng YD, Frenkel D, Li J, Sidman RL, Walsh CA, Snyder EY, Khoury SJ. Directed migration of neural stem cells to sites of CNS injury by the stromal cell-derived factor 1alpha/CXC chemokine receptor 4 pathway. Proc Natl Acad Sci U S A. 2004; 101(52):18117–18122. [PubMed: 15608062]

Kaufmann WE, Moser HW. Dendritic anomalies in disorders associated with mental retardation. Cereb Cortex. 2000; 10(10):981–991. [PubMed: 11007549]

Kolb B, Whishaw IQ. Brain plasticity and behavior. Annual review of psychology. 1998; 49:43–64.

Levinson JN, Chery N, Huang K, Wong TP, Gerrow K, Kang R, Prange O, Wang YT, El-Husseini A. Neuroligins mediate excitatory and inhibitory synapse formation: involvement of PSD-95 and neurexin-1beta in neuroligin-induced synaptic specificity. J Biol Chem. 2005; 280(17):17312–17319. [PubMed: 15723836]

Limoli CL, Giedzinski E, Baure J, Rola R, Fike JR. Redox changes induced in hippocampal precursor cells by heavy ion irradiation. Radiat Environ Biophys. 2007; 46(2):167–172. [PubMed: 17103219]

Lonart G, Parris B, Johnson AM, Miles S, Sanford LD, Singletary SJ, Britten RA. Executive function in rats is impaired by low (20 cGy) doses of 1 GeV/u (56)Fe particles. Radiat Res. 2012; 178(4):289–294. [PubMed: 22880624]

Markesbery WR. Oxidative stress hypothesis in Alzheimer's disease. Free Radic Biol Med. 1997; 23(1):134–147. [PubMed: 9165306]

Matsuzaki M, Honkura N, Ellis-Davies GC, Kasai H. Structural basis of long-term potentiation in single dendritic spines. Nature. 2004; 429(6993):761–766. [PubMed: 15190253]

Meyers CA. Neurocognitive dysfunction in cancer patients. Oncology (Williston Park). 2000; 14(1):75–79. discussion 79, 81–72, 85. [PubMed: 10680150]

Miller ED, Derenchuk V, Das IJ, Johnstone PA. Impact of proton beam availability on patient treatment schedule in radiation oncology. Journal of applied clinical medical physics / American College of Medical Physics. 2012; 13(6):3968. [PubMed: 23149788]

Mizumatsu S, Monje M, Morhardt D, Rola R, Palmer T, Fike J. Extreme sensitivity of adult neurogenesis to low doses of X-irradiation. Cancer Res. 2003; 63(14):4021–4027. [PubMed: 12874001]

Mohan R, Bortfeld T. Proton therapy: clinical gains through current and future treatment programs. Frontiers of radiation therapy and oncology. 2011; 43:440–464. [PubMed: 21625168]

Parihar VK, Limoli CL. Cranial irradiation compromises neuronal architecture in the hippocampus. Proc Natl Acad Sci U S A. 2013; 110(31):12822–12827. [PubMed: 23858442]

Pfeiffer BE, Huber KM. The state of synapses in fragile X syndrome. Neuroscientist. 2009; 15(5):549–567. [PubMed: 19325170]

Preissmann D, Leuba G, Savary C, Vernay A, Kraftsik R, Riederer IM, Schenk F, Riederer BM, Savioz A. Increased postsynaptic density protein-95 expression in the frontal cortex of aged cognitively impaired rats. Exp Biol Med (Maywood). 2012; 237(11):1331–1340. [PubMed: 23239444]

Saury JM, Emanuelson I. Cognitive consequences of the treatment of medulloblastoma among children. Pediatric neurology. 2011; 44(1):21–30. [PubMed: 21147383]

Selkoe DJ. Alzheimer's disease is a synaptic failure. Science. 2002; 298(5594):789–791. [PubMed: 12399581]

Takashima S, Iida K, Mito T, Arima M. Dendritic and histochemical development and ageing in patients with Down's syndrome. Journal of intellectual disability research : JIDR. 1994; 38(Pt 3):265–273. [PubMed: 8061472]

Terry RD, Peck A, DeTeresa R, Schechter R, Horoupian DS. Some morphometric aspects of the brain in senile dementia of the Alzheimer type. Annals of neurology. 1981; 10(2):184–192. [PubMed: 7283403]

Tronel S, Fabre A, Charrier V, Oliet SH, Gage FH, Abrous DN. Spatial learning sculpts the dendritic arbor of adult-born hippocampal neurons. Proc Natl Acad Sci U S A. 2010; 107(17):7963–7968. [PubMed: 20375283]

Tseng BP, Giedzinski E, Izadi A, Suarez T, Lan ML, Tran KK, Acharya MM, Nelson GA, Raber J, Parihar VK, Limoli CL. Functional consequences of radiation-induced oxidative stress in cultured neural stem cells and the brain exposed to charged particle irradiation. Antioxidants & redox signaling. 2013 In Press.

Urbanska M, Swiech L, Jaworski J. Developmental plasticity of the dendritic compartment: focus on the cytoskeleton. Advances in experimental medicine and biology. 2012; 970:265–284. [PubMed: 22351060]

van Praag H, Schinder AF, Christie BR, Toni N, Palmer TD, Gage FH. Functional neurogenesis in the adult hippocampus. Nature. 2002; 415(6875):1030–1034. [PubMed: 11875571]

van Spronsen M, Hoogenraad CC. Synapse pathology in psychiatric and neurologic disease. Current neurology and neuroscience reports. 2010; 10(3):207–214. [PubMed: 20425036]

Yoshihara Y, De Roo M, Muller D. Dendritic spine formation and stabilization. Curr Opin Neurobiol. 2009; 19(2):146–153. [PubMed: 19523814]

Yuste R, Bonhoeffer T. Morphological changes in dendritic spines associated with long-term synaptic plasticity. Annual review of neuroscience. 2001; 24:1071–1089.

Yuste R, Bonhoeffer T. Genesis of dendritic spines: insights from ultrastructural and imaging studies. Nat Rev Neurosci. 2004; 5(1):24–34. [PubMed: 14708001]

Zhou C, Huang Y, Przedborski S. Oxidative stress in Parkinson's disease: a mechanism of pathogenic and therapeutic significance. Ann N Y Acad Sci. 2008; 1147:93–104. [PubMed: 19076434]
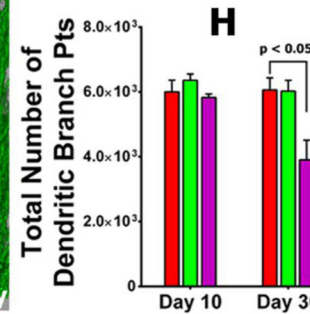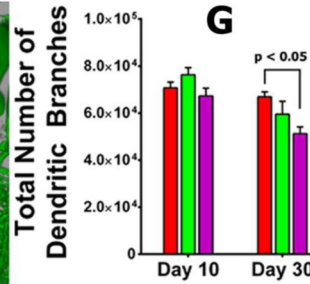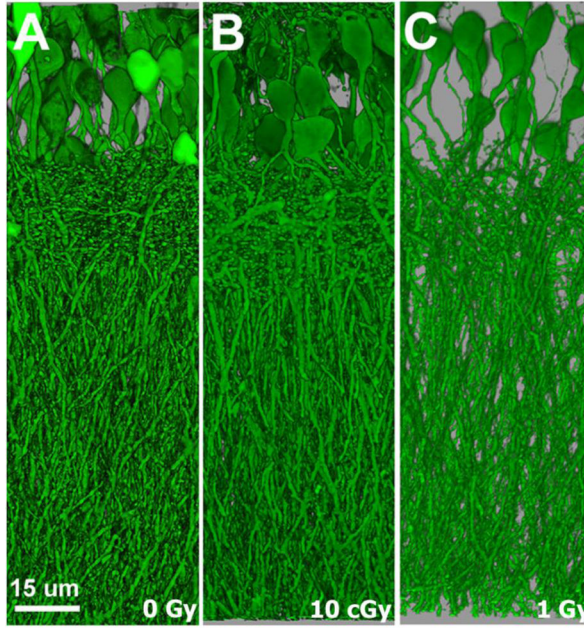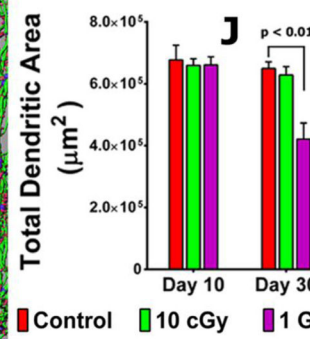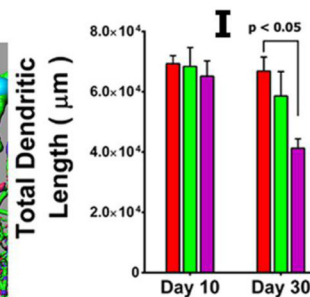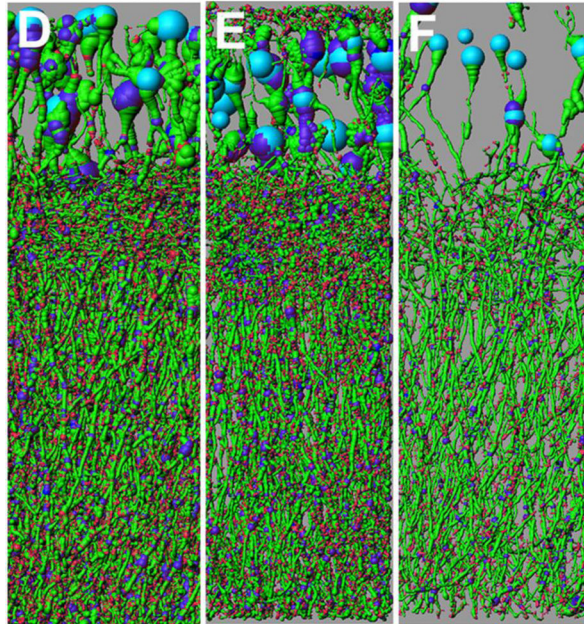
Fig. 1. Reduced dendritic complexity of granule cell layer (GCL) neurons 10 and 30 days after irradiation

(A–C), Examples of deconvoluted eGFP positive GCL neurons showing dendrites orientated vertically and traversing the molecular layer (ML). (D–F), Deconvoluted 3D reconstructed images of A–C respectively, with dendrites containing spines projecting into the ML (sky blue, cell body; green, dendrites; blue, branch points; red, spines). (G) dendritic branching numbers, (H) dendritic branch points, (I) total dendritic length, and (J) total dendritic area quantified at 10 and 30 days after exposure to 0.1 and 1.0 Gy.
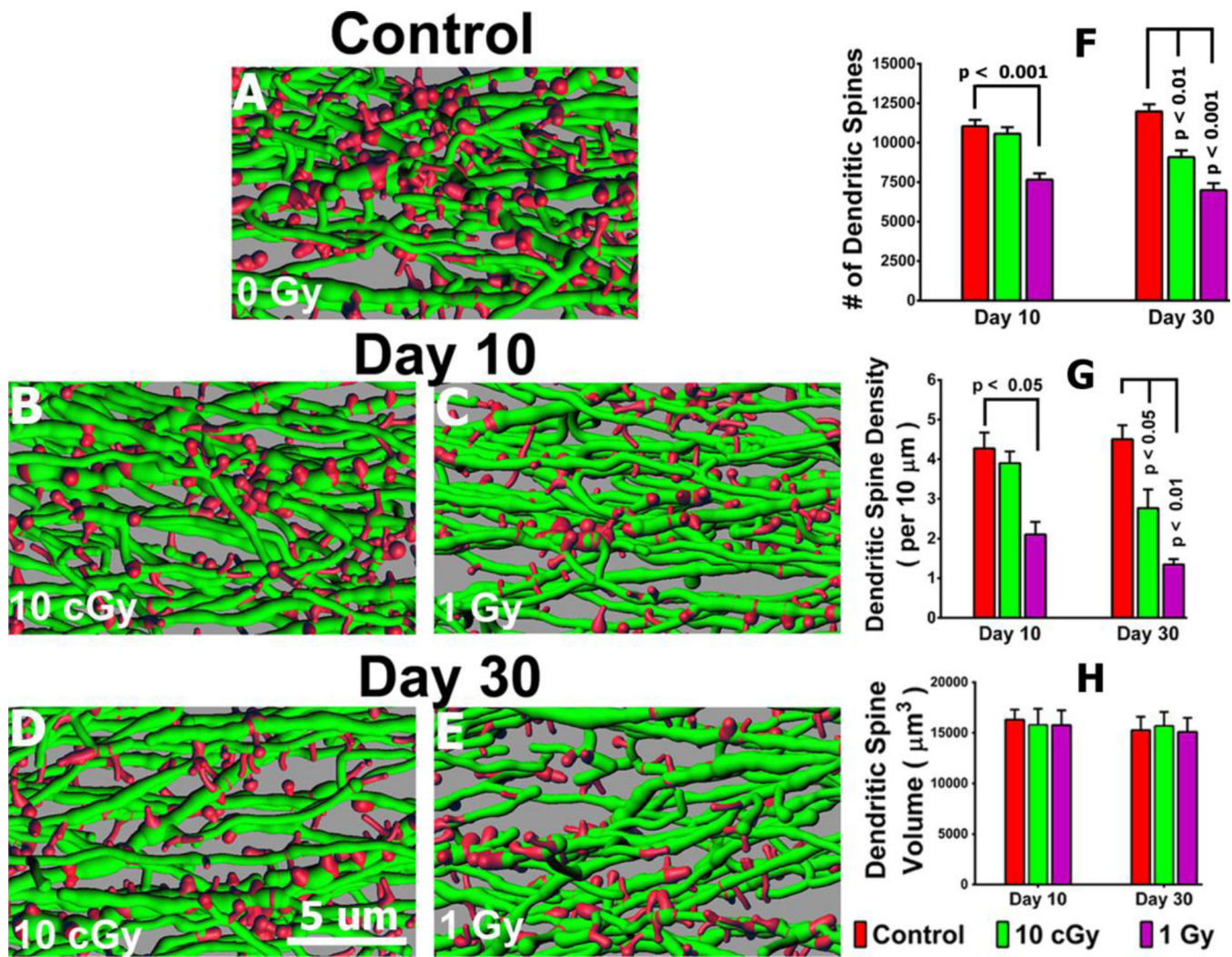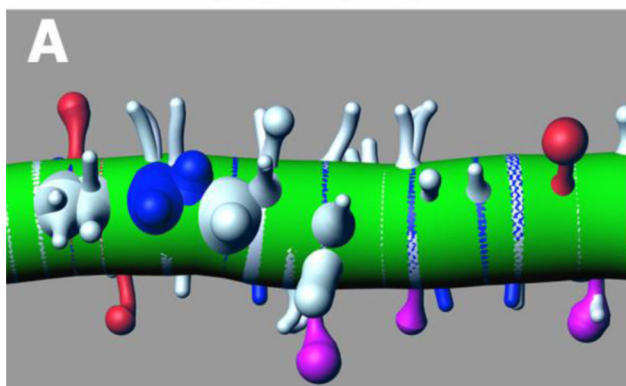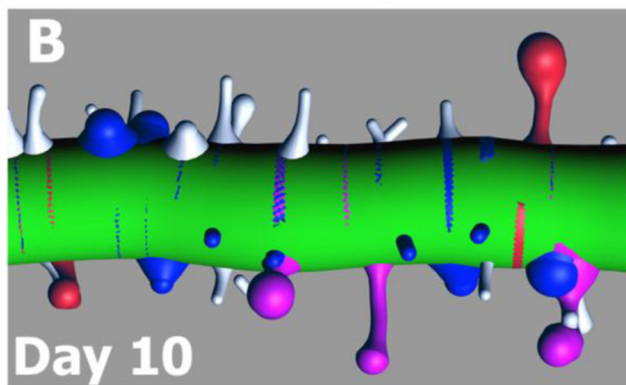
Fig. 2. Radiation-induced reductions in dendrite spine density
(A–E), Representative images 3D reconstructed dendritic segments (green) containing spines (red). (F–H), Quantified dendritic spine parameters including spine number (F), spine density (G) and spine volume (H) along GCL neurons 10 or 30 days after irradiation.
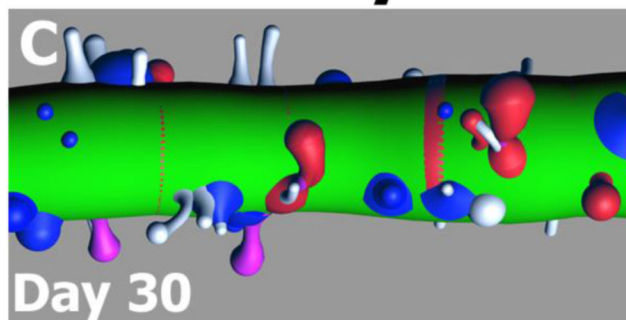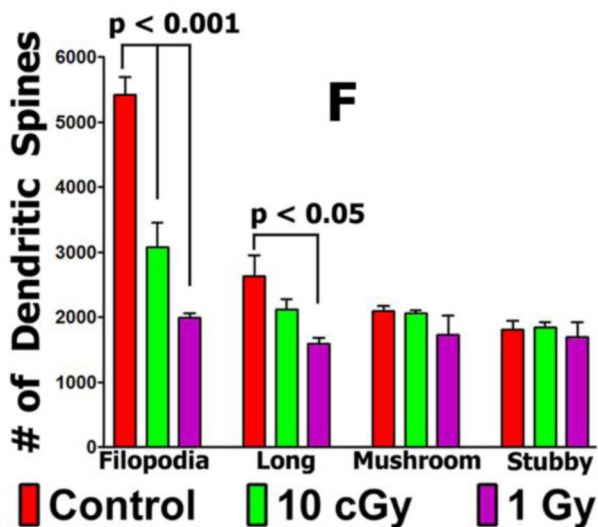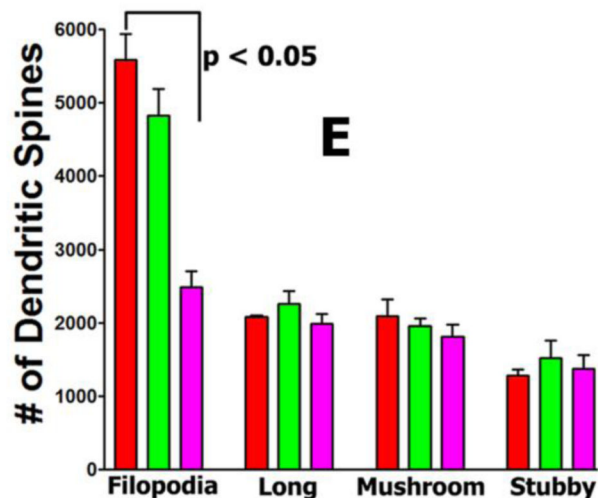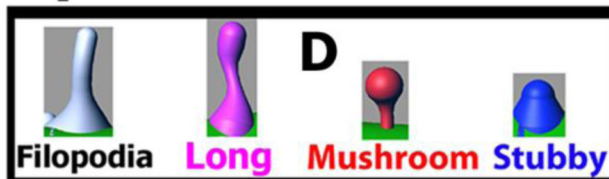
Fig. 3. Radiation-induced changes in the number of morphologically distinct spines
Reconstructed dendritic segments showing the radiation-induced reductions in filopodia
(white, A–C) along with other spine types after irradiation, using the color-coded
classification shown (D). (E–F), Quantified spine types including immature filopodia along
with more mature long, mushroom and stubby morphologies 10 (E) and 30 (F) days
following irradiation.

Fig. 4. Up-regulation of PSD-95 expression following irradiation
Fluorescence micrographs show that irradiation leads to increased expression of PSD-95 puncta (red) in GCL neurons of the ML at both 10 (C, D) and 30 (E, F) days after irradiation compared to controls (A). (B) Quantified PSD-95 puncta at 10 and 30 days after exposure to 0.1 and 1.0 Gy.
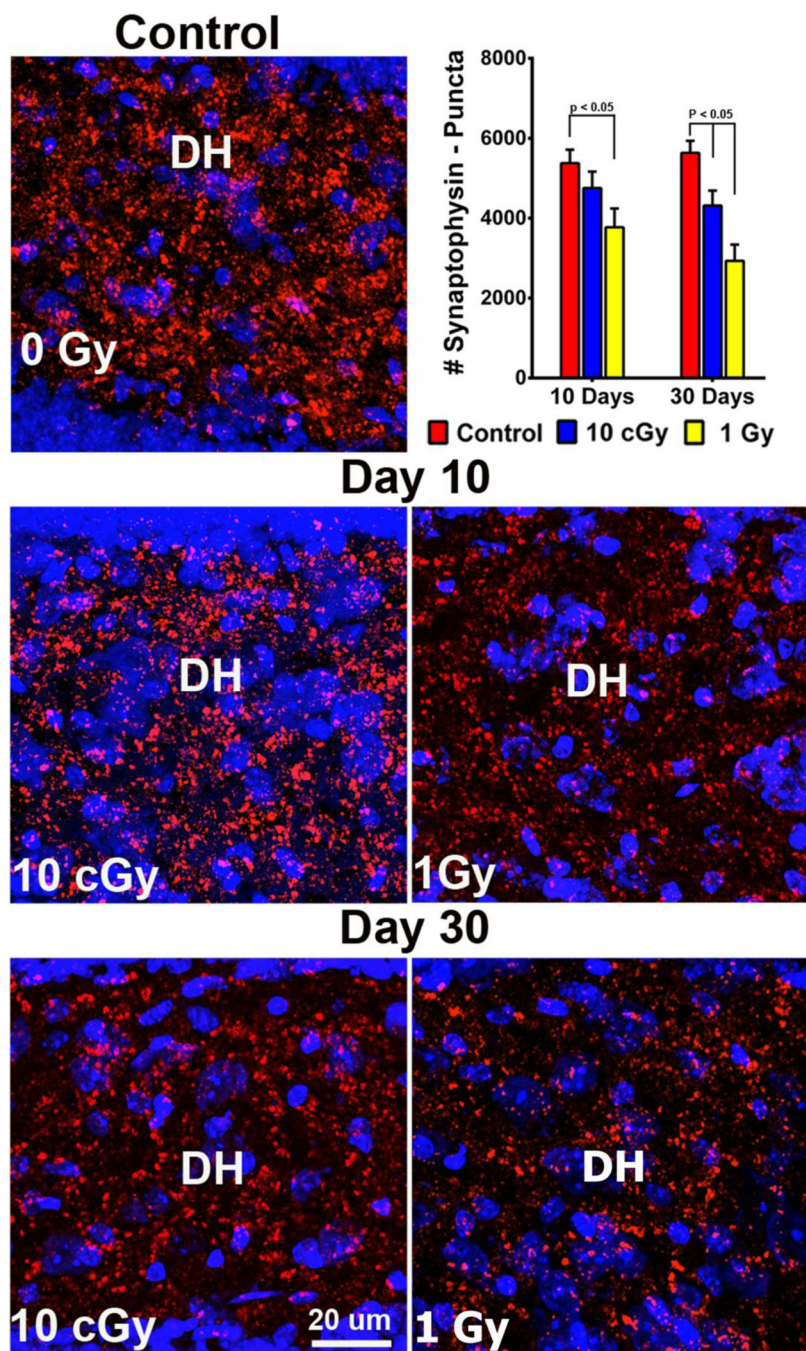
Fig. 5. Down-regulation of the presynaptic marker synaptophysin following irradiation
Representative images of synaptophysin expression show reduced expression in the DH
(blue, cell bodies stained with DAPI; red, synaptophysin expression) at both 10 (C, D) and
30 (E, F) days after irradiation compared to controls (A). (B) Quantified synaptophysin
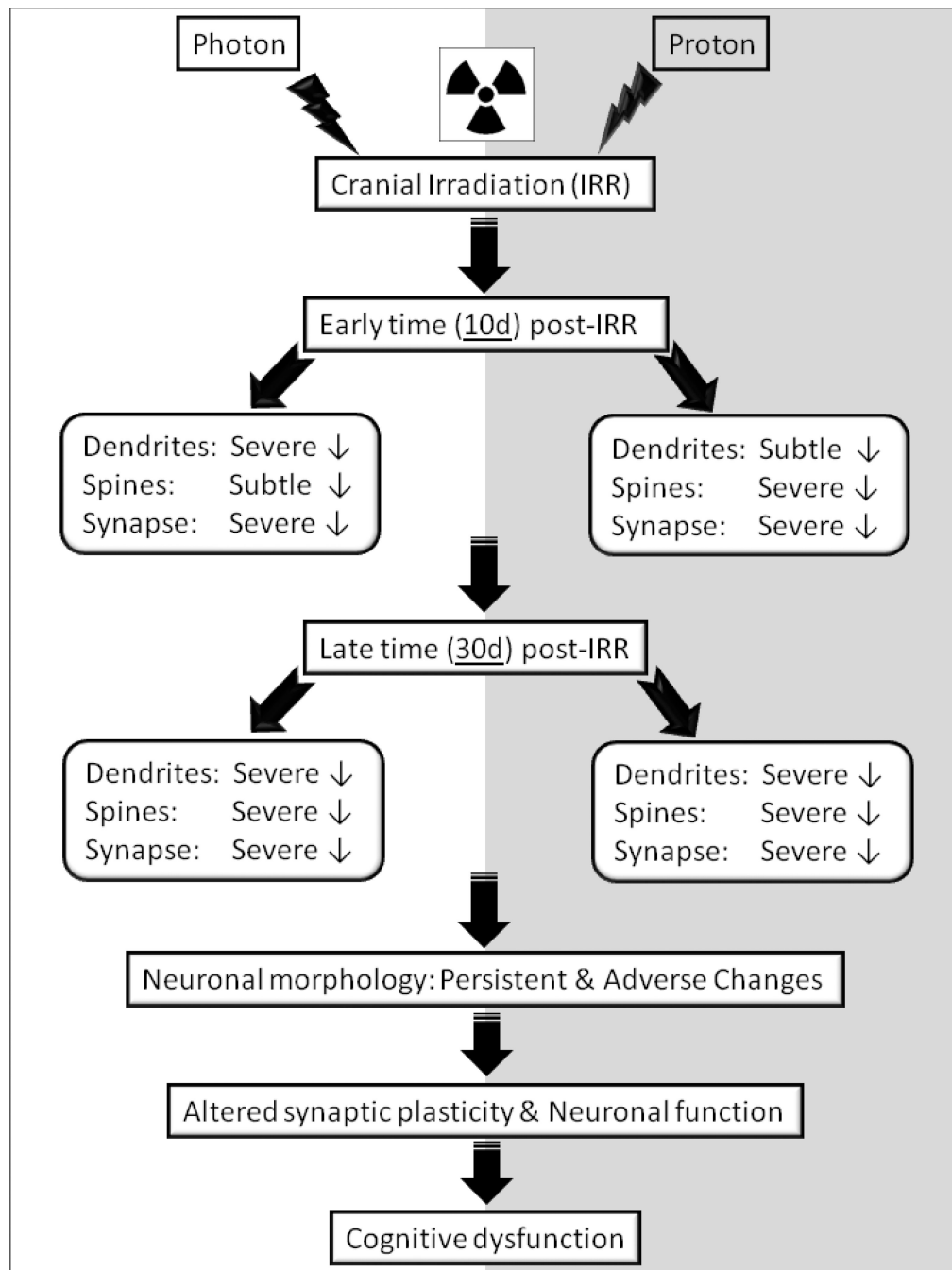staining at 10 and 30 days after exposure to 0.1 and 1.0 Gy.

Fig. 6.
Schematic representation of consequences of photon and proton irradiation-induced deterioration of structural and synaptic parameters of hippocampal neurons that eventually perpetuate into cognitive dysfucntion.

Table 1

Altered structural and synaptic plasticity induced after photon or hadron therapy

Structural Parameter*	Endpoint	10 days after 1Gy		30 days after 1 Gy	
		Photon	Proton	Photon	Proton
Dendrites	Branch no.	↓33	↓5	↓49	↓33
	Branch points	↓29	↓3	↓50	↓35
	Length	↓31	↓7	↓68	↓38
	Area	↓26	↓7	↓77	↓35
Spines	Spine no.	↓4	↓31	↓30	↓42
	Density	↓9	↓50	↓41	↓70
	Volume	↓4	↓3	↓7	↓2
Spine types	No. of Fliopodia	↓4	↓66	↓40	↓73
	No. of Long spines	↑10	↓5	↓10	↓41
	No. of Mushroom	↓7	↓14	↓6	↓18
	No. of Stubby	↑7	↑7	↓8	↓7
Post-synaptic protein	PSD95	↑71	↑59	↑171	↑110
Pre-synaptic protein	Synaptophysin	↓39	↓29	↓31	↓48

*
Numbers represent relative change (%) compared to unirradiated controls. Arrows indicate increase (↑) or decrease (↓) in the value of each parameter. Photon data derived from reference: Parihar and Limoli, *PNAS*, 2013.